2022

The effect of autophagy related protein 10 and its mutants on autophagic activity

SK Nadia Rahman Silvia

The effect of autophagy related protein 10 and its mutants on autophagic activity

Abstract

Autophagy is the cellular degradation process in which cellular contents are encapsulated by double-membrane vesicles, autophagosomes, and delivered to the vacuole to be degraded and recycled. This process is important for cell health and homeostasis. There are approximately 32 different autophagy-related proteins involved. Atg10 is an enzyme that may affect overall autophagic activity by changing autophagosome size and/or number. Our goal is to find mutants that cause a significant, partial loss in Atg10's activity by mutating some residues near the active site and testing the functionality of these mutants by performing western blots and enzymatic assays. Here we show that the Atg10 mutants H131A and Y73Q retain autophagic activity with no significant loss in the function of Atg10.

Degree Type

Open Access Senior Honors Thesis

Department or School

Chemistry

First Advisor

Dr. Steven Backues, PhD

Second Advisor

Dr. Hedeel Evans, PhD

Third Advisor

Dr. Deborah Heyl-Clegg, PhD

Subject Categories

Chemistry

THE EFFECT OF AUTOPHAGY RELATED PROTEIN 10 AND ITS MUTANTS ON AUTOPHAGIC ACTIVITY

By

SK. Nadia Rahman Silvia

A Senior Thesis Submitted to The Honors College at

Eastern Michigan University

in Partial Fulfillment of the Requirements for Graduation

with Honors in Chemistry

Approved at Ypsilanti, Michigan, on this date: April 6, 2022

Supervising Instructor:	Steven Backues Dr. Steven Backues, PhD	Date:	3/31/2021
Departmental Honors Advisor:	Hedeel Evans Dr. Hedeel Evans, PhD	Date:	31 March 2022
Department Head:	Deborah Heyl-Clegg Dr. Deborah Heyl-Clegg, PhD	Date:	March 31, 2022
Dean, Honors College:	Ann R. Eisenberg Dr. Ann R. Eisenberg, PhD	Date:	April 6, 2022

Table of Contents

Abstract

Autophagy is the cellular degradation process in which cellular contents are encapsulated by double-membrane vesicles, autophagosomes, and delivered to the vacuole to be degraded and recycled. This process is important for cell health and homeostasis. There are approximately 32 different autophagy-related proteins involved. Atg10 is an enzyme that may affect overall autophagic activity by changing autophagosome size and/or number. Our goal is to find mutants that cause a significant, partial loss in Atg10's activity by mutating some residues near the active site and testing the functionality of these mutants by performing western blots and enzymatic assays. Here we show that the Atg10 mutants H131A and Y73Q retain autophagic activity with no significant loss in the function of Atg10.

Introduction

Macroautophagy, commonly known as autophagy, is the "self-eating" process that our body undergoes to degrade cellular components within eukaryotes. It promotes cellular health and maintains homeostasis, the constant internal environment of our body (Ryter et al., 2013). An autophagosome is a double-membrane vesicle that collects cytosol and fuses with the lysosome (or vacuole in yeast and plants), a compartment containing lysosomal hydrolases that break down the vesicle and its contents (Lőrincz & Juhász, 2020).The proteins from the cytosol are degraded and reused (N. N. Noda & Inagaki, 2015). This process can also come into play to break down pathogens or defective cell organelles. There are approximately 30 different autophagy (ATG) related proteins involved (Xie & Klionsky, 2007). If the process is disrupted and fails to take place, it results in detrimental effects, such as neurodegeneration. This results in diseases like Parkinson's and Alzheimer's due to build-up of protein aggregates and other cellular debris (Scrivo et al., 2018; Wu et al., 2018). Additionally, aging is related to reduced

levels of autophagy (Escobar et al., 2019). Therefore, understanding the process of autophagy by understanding the role of autophagy-related proteins will help future research that will develop effective therapeutic agents to benefit human health. *Saccharomyces cerevisiae*, baker's yeast, is the primary model used in understanding the process of autophagy. This is because the majority of autophagic proteins and their processes are conserved from yeast to humans (Reggiori & Klionsky, 2013).

There are two different types of autophagy: selective and nonselective. Selective autophagy targets and envelops cargo materials, such as aggregation-prone proteins, into autophagosomes. On the contrary, nonselective autophagy is stimulated by nutrient deprivation. It involves uptake of a random cell body into autophagosomes and eventually degrades and recycles back into the cytoplasm (see Figure 1). It is responsible for protein turnover and helps the cells to survive starvation (Gatica et al., 2018).

Atg proteins are upregulated under nutrient depletion conditions, and many studies have investigated the effect of Atg proteins on autophagic flux. Autophagic flux is the rate of autophagic degradation. It involves the uptake of the cell body into autophagosomes. Therefore, both the size and/or the number of autophagosomes affect autophagic flux. Understanding the effect of Atg proteins on autophagosome size and number can provide insight into the process of autophagic activity (Cawthon et al., 2018).

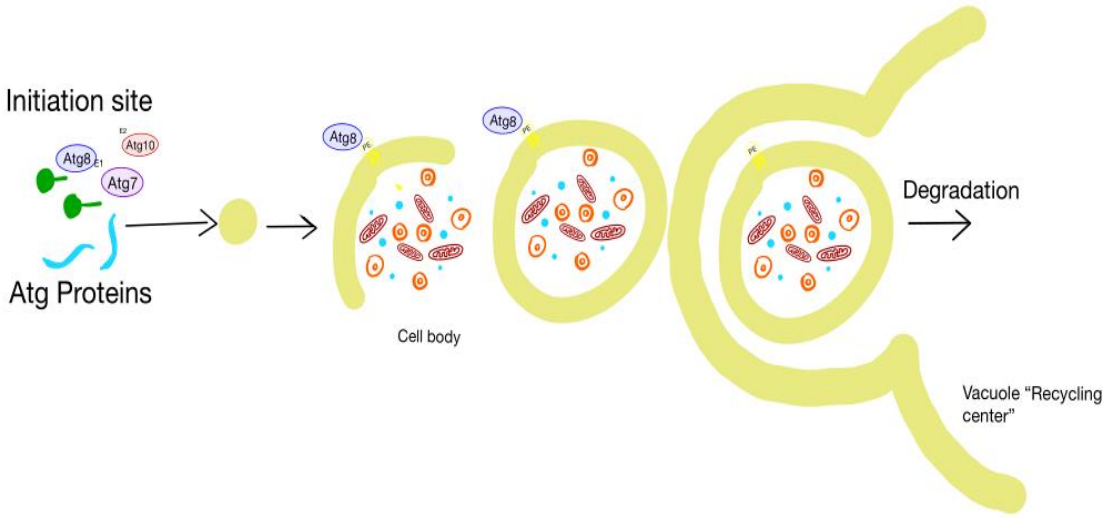

Figure 1: *Process of nonselective autophagy.* Atg7, Atg8, and Atg10 are proteins necessary for autophagy. The Atg proteins are recruited at the initiation site. The autophagic membrane encapsulates the cell body, and Atg8 facilitates expansion. This results in the formation of an autophagosome, which eventually fuses with the vacuole for degradation. The thick yellow line represents the lipid membrane. Diagram made using GoodNotes5.

Many research studies have used the Atg8-PE conjugation system to investigate the process of autophagy (Geng & Klionsky, 2008; Nair et al., 2012; Martens & Fracchiolla, 2020). Atg8 and Atg12, ubiquitin-like proteins, are vital for the formation of autophagosomes. Atg8 is conjugated to the membrane lipid phosphatidylethanolamine (PE) and facilitates the expansion of autophagic bodies or autophagosomes. Atg12 is a component of the Atg12-Atg5-Atg16 complex. This is the E3 enzyme for the Atg8-PE conjugation cascade (Matoba & Noda, 2021).

The first step of the Atg8-PE conjugation cascade involves the E1 enzyme, Atg7, that activates the E2 conjugating enzymes, Atg3 and Atg10. Atg10 conjugates the Atg12-Atg5-Atg16 complex, and this complex upregulates the activity of Atg3, which conjugates Atg8 to lipid PE (Phosphatidylethanolamine). Atg7 initiates this pathway, and Atg8 attached to PE is the end-product. A recent study has shown that Atg7 affects both the size and number of autophagosomes (Cawthon et al., 2018). Another study has shown that Atg8 affects only the size

of autophagosomes (Xie et al., 2008). So, we hypothesized that the intermediate proteins, Atg3 and Atg10, affect either number or both the size and number of the autophagosomes. Therefore, understanding the role of Atg3 and Atg10 is crucial to understanding the autophagic pathway.

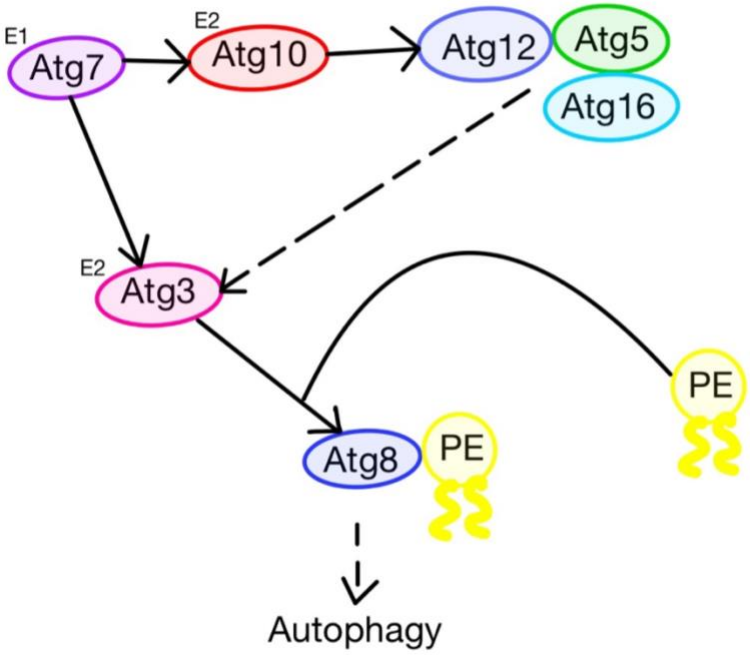

Figure 2: *The autophagic pathway by which Atg10 helps attach Atg8 to Lipid PE.* Atg7 activates Atg10 and Atg3. Atg10 conjugates Atg12-5-16 complex. Atg12-5-16 complex upregulates Atg3 by causing a conformational change in Atg3. Atg3 conjugates Atg8 to lipid PE. Diagram made using GoodNotes5.

The Inagaki lab performed an extensive study to understand the formation of Atg12-Atg5 conjugate by Atg10 (Yamaguchi et al., 2012). They reported the crystal structures of Atg10 homolog from Kluyeromyces marxianus (Km). Through NMR experiments and in vitro mutational assays, they found some residues relevant for the interaction of KmAtg10 with KmAtg5. These residues were located near the active site of the catalytic cysteine, Cys116. So, they mutated and tested the residues that showed significantly reduced levels of Atg12-Atg5 conjugate. They also generated ScAtg10 (Saccharomyces Cerevisiae) mutants corresponding to

KmAtg10 mutants. They have shown reduced levels of Atg12-Atg5 conjugation in knockout cells expressing Tyrosine 73 and Histidine 131 mutants (Yamaguchi et al., 2012). We ***hypothesize*** that creating these mutations in Atg10 would result in a knockdown effect in the protein function and result in reduced formation levels of Atg8-PE and partial loss in the overall autophagic activity. Thus, these mutations could be used to understand the role of Atg10 on autophagosome size and number.

Material and Methods

Yeast and Bacterial Culture Conditions

For this research, both yeast and bacterial cultures were needed. Yeast cultures were grown in YPD (1% w/v yeast extract, 2% w/v peptone, 2% w/v glucose) and shaken at 300 rpm at 30°C. Starvation was induced by resuspending cells in SD-N media (0.69 g/L YNB without amino acids or ammonium sulfates, 2% w/v glucose) and shaking at 300 rpm at 30°C for 3 hours. Bacterial cultures were grown in LB media (0.5% w/v yeast extract, 1% w/v tryptone, 1% w/v NaCl, water) shaken at 220 rpm at 37°C.

Strains

The strains used in this study are listed in Table 1. The *atg10Δ* and *Atg10-PA* strains were generated using methods described by Longtine et al. (1998). These strains were verified by PCR with primers flanking the ATG10 locus. All PCR was performed using the BioRad MyCyclerTM thermal cycler, using New England Biolabs Phusion HF polymerase (NEB). The PCR product was purified using the NucleoSpin PCR Clean-up kit (Machery-Nagel). Primers for PCR were obtained from Integrated DNA Technologies and are listed in Table 2. After PCR, gel electrophoresis was performed using a Horizontal Electrophoresis System from Fisher Biotech and an EC135 power supply from E-C Apparatus Corporation. All the samples were stained with gel red and imaged in BioRad ChemiDoc Imaging System.

Table 1: S. cerevisiae strains used in this study.

Strain Name	Genotype
SKB422	WLY176 SEY6210 *pho13*Δ *pho8*Δ*60*
SKB1000	WLY176 *atg10Δ::Kan*
SKB1027	WLY176 *atg10Δ::Kan::ura3-52::pRS406-Empty*
SKB1028	WLY176 *atg10Δ::Kan::ura3-52::pRS406-Atg10-PA(2)*
SKB1029	WLY176 *atg10Δ::Kan::ura3-52::pRS406-Atg10-PA(4)*
SKB1030	WLY176 *atg10Δ::Kan::ura3-52::pRS406-Atg10-PAY73Q(1)*
SKB1031	WLY176 *atg10Δ::Kan::ura3-52::pRS406-Atg10-PAY73Q(2)*
SKB1032	WLY176 *atg10Δ::Kan::ura3-52::pRS406-Atg10-PAH131A*(2)
SKB1033	WLY176 *atg10Δ::Kan::ura3-52::pRS406-Atg10-PAH131A(4)*

Atg10 knockout

The ATG10 gene was knocked out of the WLY176 yeast strain (Kanki et al., 2009) by homologous recombination using primers 399 and 434 and template plasmid *pFA6-Kan (Longtine et al., 1998)*. This process is comprised of PCR followed by gel electrophoresis. This PCR product contained homology to Atg10 and kanamycin resistance from *pFA6-Kan*, as it replaced the coding sequence for Atg10 protein by homologous recombination. Then, high-efficiency yeast transformation using the LiAc/SS carrier DNA/PEG method was used to transform the PCR product into WLY176 strain; yeast were plated onto YPD plates with 200 μl of 100 mg/mL G418 for kanamycin selection (Gietz & Schiestl, 2007). Genomic DNA from this transformation was purified and verified using primers 482 and 444, followed by gel electrophoresis.

Table 2: Primers used for PCR

Primer Number	Name	Description	Sequence
SKB398	Atg10 F2	For pringle C -terminal PA tagging, forward primer	CAGTATTTTCATATTTAGTT GGTTAGGTTATGAAGATTCA cggatccccgggttaattaa
SKB399	Atg10 R1	For pringle c-terminal PA tagging, reverse primer	gatgattgcatagtgttttaaaaagctttcct aggttaagGAATTCGAGCTCG TTTAAAC
SKB423	Atg10 p	Forwards primer for cloning 1000 bp of the ATG10 promoter 20bp homology to prs406.	acggtatcgataagctt CGAATCCAAACAACTCAAGA
SKB434	Atg10 F1	Pringle deletion of Atg10 "F1" primer (former SKB410, with 40bp homology upstream of Atg10 instead of 20bp)	aaaaaaaaaaaagggctaaaaaacagaattatca gacttgCGGATCCCCGGGTTAATT AA
SKB444	Pringle Internal Checking R	Primer annealing to the pFA6A (pringle) fragment (reverse of F1 sequence). Use with a forwards primer upstream of a gene to check for deletion of that gene via pringle method)	TTAATTAACCCGGGGATCCG
SKB481	Atg10 seq +200 bp rev	Internal reverse Atg10 sequencing primer	GGGCTCGTTATATACTTTTGAA TATGTA
SKB482	Atg10 -324 new seq flanking Forward	Sequencing primer starting 325 bp upstream of Atg10 start codon, reading forwards	GGCGACAAGGTGTTCTAGT
SKB488	Atg10 mut H131A F	Mutates H131A, CAT to GCA. Use with SKB488	TATTCTTTCGCACCATGCGATA CATCATGTATAGTAGGTGA
SKB489	Atg10 mut H131A R	Mutates H131A, CAT to GCA. Use with SKB487	TATCGCATGGTGCGAAAGAAT ACCAAACGCTACCT
SKB490	NEW Atg10 mut Y73Q F	Mutates Y73Q, TAT to CAA. Use with SKB 491	CAAAAGTACAAAACGAGCCCT TACTACTTT
SKB491	NEW Atg10 mut Y73Q R	Mutates Y73Q, TAT to CAA. Use with SKB 490	GGGCTCGTTTTGTACTTTTGAA TATGTAAG

Atg10-PA

Our protein of interest, Atg10, was PA tagged on its C-terminus to be able to see the presence of Atg10 via western blot. Atg10 has homology to the vector, *pFA6-PA*. *Atg10-PA* was driven by native ATG10 promoter. An Atg10-directed PA-kan was created using pringle primers, Atg10 F2 (SKB398) and Atg10 R1 (SKB399). The presence of Atg10-PA was verified by immunoblotting with PAP antibody. The circular vector, pRS406, was linearized by EcoRI and HindII restriction enzymes to create cuts in its multiple cloning site. Using primers 423 and 399, *Atg10-PA* was amplified and inserted into *pRS406* by In-fusion Eco Dry Cloning Kit. The product was transformed into stellar competent *E. coli* cells and plated on LB plus 50 μg/ml

carbenicillin selective media. Then, *pRS406-Atg10-PA* plasmids were purified by DNA miniprep. The presence of Atg10-PA was verified by sanger sequencing at the University of Michigan Genomics Core. Once verified, the plasmid was linearized by Stu1 restriction enzyme in the URA3 gene, integrated into WLY176 *atg10Δ* yeast cells, and selected for by plating on SMD-ura plates (0.69% w/v yeast nitrogen base, 0.5% w/v casamino acids, 2.4% w/v agar, 1X amino acid dropout stock, 2% glucose) (Gietz & Schiestl, 2007). The presence of PA tag was further verified by PA immunoblotting. The functionality of the PA tagged strain was investigated by Ape1 and Atg8-PE western blot, and an ALP assay (described below).

Atg10 mutants Y73Q and H131A

Using site-directed mutagenesis, the Atg10 mutants, pRS406-Atg10-PA^{Y73Q} and pRS406-Atg10-PA^{H131A}, were created by PCR followed by gel electrophoresis. Primers 490 and 491 were used to amplify the Y73Q mutant plasmid by mutating TAT to CAG. Primers 488 and 499 were used to amplify the H131A mutant plasmid by mutating CAT to GCA. The template for both reactions was unmutated pRS406-Atg10-PA. After the mutants were created, the plasmids were circularized by In-fusion Eco Dry Cloning Kit. The presence of the desired ions in pRS406-Atg10-PA^{Y73Q} and pRS406-Atg10-PA^{H131A}, and the accuracy of those plasmids, were verified by sanger sequencing at the University of Michigan Genomics Core. Once verified, the plasmids were linearized by making a cut at the URA3 gene and integrated into WLY176 *atg10Δ* yeast cells as described for Atg10-PA above.

TCA Precipitation

Yeast cells were grown in log phase in YPD. Two sets of 1 OD cells were analyzed. The first set of samples (0 hour) was harvested by centrifugation for 5 minutes, 2000 g, resuspended in 10% ice cold trichloroacetic acid (TCA), and incubated for 20 minutes on ice. Then, the samples were centrifuged at max speed in 4°C cold room for 5 minutes, and the resulting pellet

was washed in ice-cold acetone, air dried for at least 15 minutes, and stored in -20°C. The second set of samples was washed with sterile water and starved in SD-N for 3 hours. Then, these cells were harvested, and TCA precipitated the same way as the set one (0 hour). Both sets of samples were then resuspended in 0.2 per µl of 1XSSB with 0.25M Tris pH 6.8 before western blotting.

Western Blotting

The cells in SSB were treated with glass beads for lysis using a Disruptor Genie for 5 minutes at 4°C, then heated for 5 minutes at 95°C, and centrifuged at 13000 g at room temperature (RT). A 10 µL sample was loaded in each lane of a 10-lane hand-poured SDS-PAGE gel. Then, the western blot was performed using the standard protocol of SDS-PAGE and tank transfer. The transfer was performed on Hydrophilic polyvinylidene fluoride (PVDF) membrane (Millipore) soaked in EtOH (95% v/v ethanol) followed by water and Towbin (15 mM Tris, 192 mM glycine pH 8.3). Blocking and antibody treatment was done in 4% w/v nonfat dry milk in TBST (1X Tris-Buffered Saline, 0.1% Tween). Immobilon Crescendo Western HRP substrate Millipore reagent was used to detect the proteins, and a BioRad Chemidoc XRS+ system was used to image the blots.

To examine expression level of PA tagged Atg10 proteins, a PA immunoblotting technique was used to detect the antigen-antibody interaction. For this SDS-PAGE, 12.5% acrylamide gels comprising of a resolving gel and a stacking gel were used. After the tank transfer, the PVDF membrane was cut between 35-48 KDa (a little above 35 KDa), as we expected to see Atg10-PA around 33.5 KDa and pGK1 loading control around 45 KDa. The top half of the membrane was probed overnight at 4°C in 1:10000 anti Pgk1, then probed for 1 hour in 1:5000 mouse-α-rabbit secondary HRP at RT. The bottom half of the membrane was probed in 1:500 Peroxidase anti-Peroxidase (PAP) antibody for 1 hour at RT

To examine the autophagic activity of Atg10 mutant and tagged strains, an Atg8-PE immunoblotting technique was used to detect the effect of Atg10 mutant and tagged strains on the Atg8-PE conjugation. To run this SDS-PAGE, 13% urea resolving gels (45 mM urea 6.5% Polyacrylamide, 375 mM Tris-HCl pH=8.8, 0.1% SDS, 0.1% APS, .017% TEMED) were used for better band separation, and 5% acrylamide stacking gels (5% v/v Polyacrylamide, 125 mM Tris-HCl pH=6.8, 0.1% SDS, 0.1% APS, 0.1% TEMED) were used for loading samples. After the tank transfer, the PVDF membrane was cut between 17-20 KDa, as we expected to see Atg8-PE at 14 KDa. The top portion of membrane was then discarded, and the bottom portion was probed overnight at 4°C in 1:1000 rabbit-α-Atg8 primary antibody followed by goat-α-rabbit 2° HRP for 1 hour at RT.

To further verify the autophagic activity of the Atg10 mutant and tagged strains, an Ape1 immunoblotting technique was used to measure the levels of Ape1 processing. For this procedure, the membrane was cut at 75 KDa after the tank transfer process of western blot. The top portion was discarded, and the bottom portion was probed overnight at 4°C, in 1:5000 rabbit-α-Ape1, followed by 1:5000 goat-α-rabbit 2° HRP for 1 hour at RT.

ALP Assay

To quantify the autophagic activity of Atg10 mutants and tagged strains, an ALP assay was performed. The ALP assay is performed in strains with the *pho8Δ60* mutation. In these strains, the alkaline phosphatase Pho8 lacks the 60 amino acid signal sequence so that it cannot be transported to the vacuole via cotranslational import into the endoplasmic reticulum and so the only other way it can get to the vacuole to be activated is through autophagy. This allows us to measure autophagic activity by determining the amount of activated alkaline phosphatase (T. Noda & Klionsky, 2008). In this procedure, yeast cells were grown in log phase in YPD. The 5 ODs of cells from each of the two sets were analyzed. The first set of samples (0-hour) were

resuspended in 500 μL ice cold lysis buffer (0.02 M PIPES KOH pH 6.8, 0.05 KCl, 0.1 M KOAc, 0.01 M $MgSO_4$, 0.01 mM $ZnSO_4$, 0.5% TX-100, in water) supplemented with glass beads. They were then processed using Disruptor Genie 10 minutes at 4°C followed by centrifugation for 5 minutes at 16,000 g. A 100 μL of supernatant from each sample was then treated with 400 μL of 37°C reaction buffer (0.25 M Tris-HCl pH 8.5, 0.01 M $MgSO_4$, 0.01 mM $ZnSO_4$, 0.4% TX-100, rest water) containing 0.625 mg para-nitrophenylphosphate (pNPP) for every milliliter of buffer. After 15 minutes of incubation in 30°C, the reaction was stopped with 500 μL stop buffer (1 M glycine-NaOH pH=11), and the resulting absorbance was measured at 420 nm. The solution turned yellow as the active Pho8Δ60 dephosphorylated pNPP. The second set of samples was washed with sterile water and starved in SD-N for 3 hours. They were then treated the same way as the 0-hour samples. A standardized ThermoFischer BSA assay was performed to analyze the lysate for protein quantification. Absorbances were read at 562 nm on the BioTek Synergy 2 Plate Reader.

Results

PA tagged Atg10 rescues autophagic activity like the wild type

Atg10 is a necessary component of the autophagic machinery (Yin et al., 2016). We hypothesize that Atg10 affects autophagosome size and/or number. To investigate whether Atg10 affects autophagosome size and/or number, we first created a knockout mutant, *atg10Δ*, in the WLY176 yeast strain using the homologous recombination technique to replace the ATG10 gene with a kanamycin resistance gene (Longtine et al., 1998). We verified this by PCR followed by gel electrophoresis (Figure 3A, 3B), then transformed the PCR product into the WLY176 yeast strains (Gietz & Schiestl, 2007). We created this WLY176 *atg10Δ* strain to re-transform

PA tagged Atg10 and its mutants into it. We tagged Atg10 with a protein tag, *Staphylococcal* protein A (PA), at the carboxyl terminus of Atg10 to see the expression level of Atg10 proteins via western blot. *Atg10-PA* was driven under native Atg10 promoter.

Ape1 is amino-peptidase-1, a hydrolase involved in protein degradation in the vacuole. Ape1 is present in the cytosol as a precursor form, pre-Ape1. It contains a 45 amino acid propeptide at its amino terminus and self-assembles into dodecamers, the Ape1 complex. The pre-Ape1 gets transported to the vacuole in two different pathways: non-selective autophagy and the Cvt pathway. Under nutrient-rich conditions, the Cvt pathway (a type of selective autophagy) packages and transports pre-Ape1. Under nutrient-depletion conditions, pre-Ape1 gets transported through non-selective autophagy. Likewise, autophagosomes form during nutrient deprivation conditions, and Cvt vesicles form during nutrient-rich conditions. When the Cvt vesicle fuses with the vacuole, the fusion of vesicles with the vacuole results in the formation of autophagic bodies that are eventually degraded. This degradation results in the propeptide being removed from the pre-Ape1 by a proteinase, Prb1, which generates mature Ape1 (mApe1)(Su et al., 2015; Wang & Klionsky, 2003). To further verify *Atg10-PA* strains, we immunoblotted these with anti-Ape1antibodies and measured the levels of pre-Ape1 and mApe1. As shown in figure 3C, the levels of pre-Ape1 and mApe1 generated by *Atg10-PA* were similar to the wild-type strain, WLY176. The *atg10Δ* strain was the negative control that could not generate the mApe1. We also quantified the levels of pre-Ape1 and mApe1. Upon starvation, the levels of cytoplasmic pre-Ape1 decrease, and vacuolar mApe1 increase (figure 3D), consistent with the stimulation of multiple types of autophagy by starvation conditions.

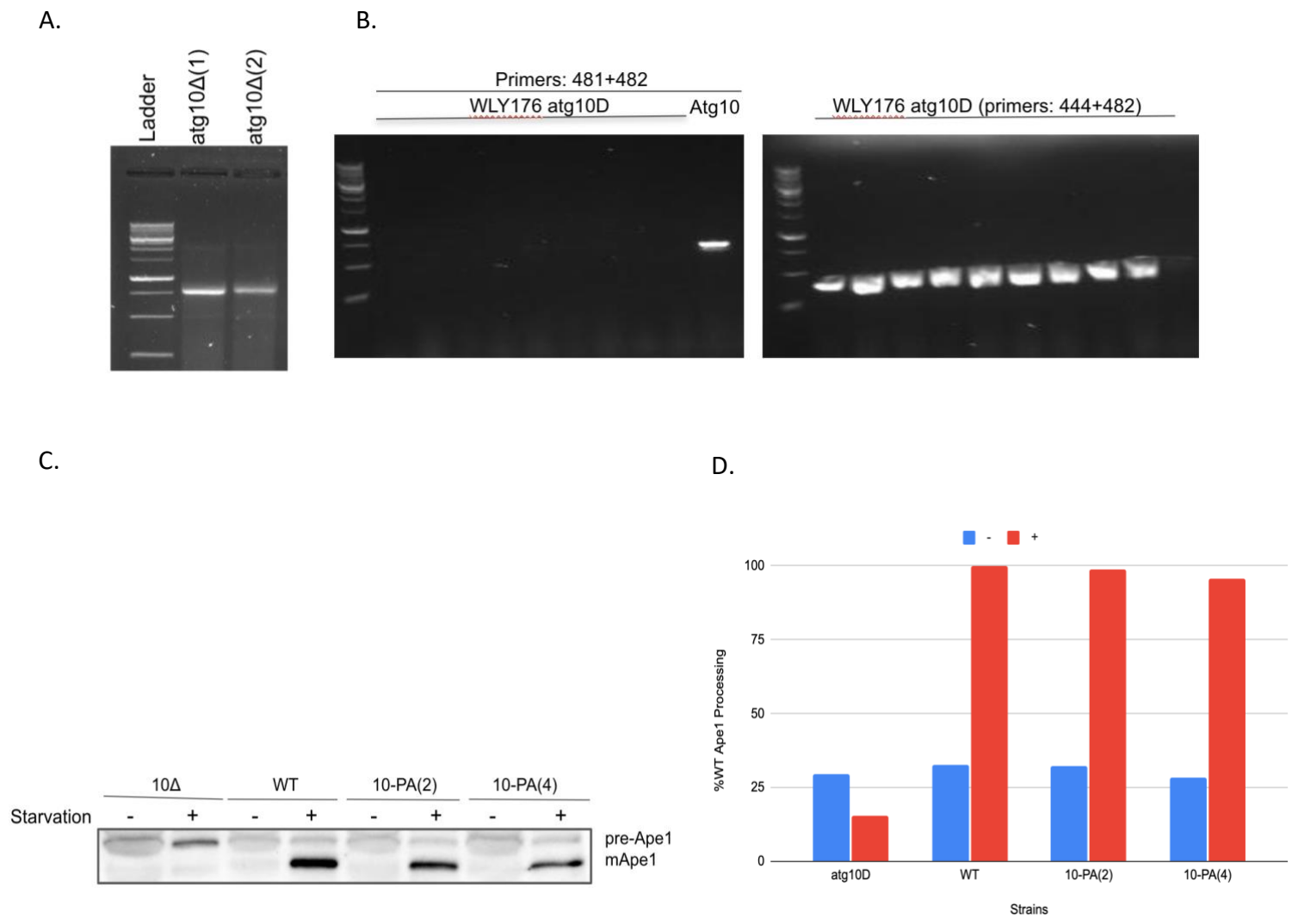

Figure 3: *Atg10-PA rescues autophagic activity like the wild type*. (A) The PCR product, atg10Δ::kan was verified by gel electrophoresis prior to transformation into WLY176 to create the atg10Δ::kan strains.. (B) The atg10Δ::kan strains were verified by genotyping PCR followed by electrophoresis. Primers 444 and 482 recognized atg10Δ, primers 481 and 482 recognized Atg10. Nine clones of WLY176 atg10Δ::kan were analyzed. The Atg10 was the positive control. (C) For analysis of Ape1 processing, WLY176 atg10Δ::kan (10Δ) was the negative control and WLY176 (WT) was the wild type, positive control. The controls, along with the PA tagged Atg10 were grown in rich medium (-) to log phase and then some samples were starved in nitrogen-starvation medium for 3 hours (+). Ape1 processing was analyzed by immunoblotting with anti-Ape1 antibodies. Cells with *Atg10-PA* were able to cleave the pre-Ape1 to form mature Ape1 (mApe1). (D) Levels of pre-Ape1 and mApe1 were quantified using ImageJ. Then the percentage of mApe1 over the total Ape1 was normalized to *Atg10-PA* starved strains.

Atg10 mutants H131A and Y73Q have no significant loss in Atg8-PE conjugation

A previous study found that mutations H131A and Y73Q in Atg10 strains decreased Atg12-Atg5 conjugation to 70% and 30% compared to the wild-type Atg10, respectively (Yamaguchi et al., 2012). Therefore, we hypothesized that these mutants would show a similar decrease in Atg8-PE conjugation and a partial loss in autophagic activity. So, we induced these mutations into our PA tagged Atg10 plasmids by using site-directed mutagenesis. The successful creation of *pRS406-Atg10-PA*^{Y73Q} (Y73Q) and *pRS406-Atg10-PA*^{H131A} (H131A), was verified by PCR and gel electrophoresis (figure 4A) followed by Sanger sequencing.

We generated multiple replicates of these plasmids and selected two independent plasmids coding for each mutation for further experiments. For mutant Y73Q, we chose plasmids Y73Q (1) and Y73Q (2). For mutant H131A, we chose plasmids H131A (2) and H131A (4). Then we transformed these mutant plasmids into WLY176 *atg10Δ* yeast strains. Atg10 is an E2 enzyme that conjugates Atg12-5-16, a complex that in turn upregulates Atg8-PE conjugation. To test the autophagic activity of these mutants, H131A and Y73Q, Atg8-PE conjugation was analyzed via western blot. Yeast cells with these mutations were grown and then starved under nitrogen depletion conditions for 3 hours. The growing and the starved cells were analyzed by immunoblotting with an anti-Atg8 antibody. The *atg10Δ* strain that lacked Atg10 could not conjugate Atg8 to the lipid PE. This strain was our negative control. The *Atg10-PA* conjugated the Atg8 to PE, and it was our positive control. As shown in figure 4B, and quantified in figure 4C, the mutants Y73Q and H131A rescued the levels of Atg8-PE conjugation similar to that of

the wild-type *Atg10-PA.* Upon starvation, the levels of cytoplasmic Atg8 decrease, and Atg8-PE increase, as Atg8 is covalently attached to the lipid PE of autophagosomes.

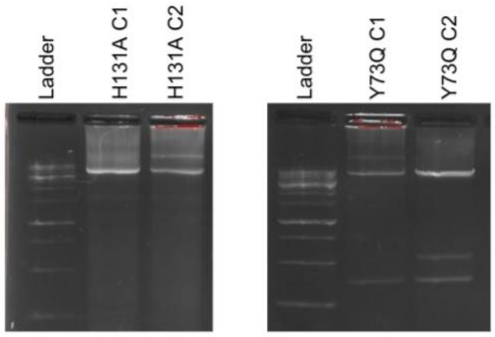

B.

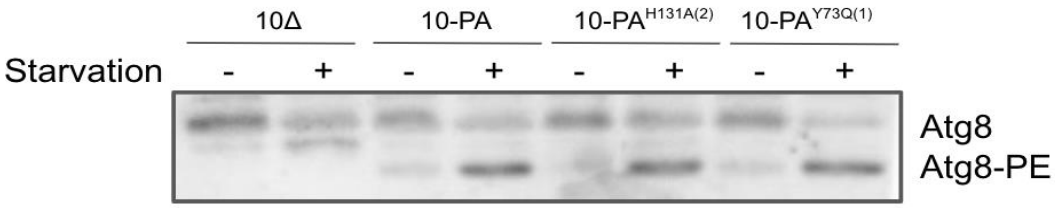

C.

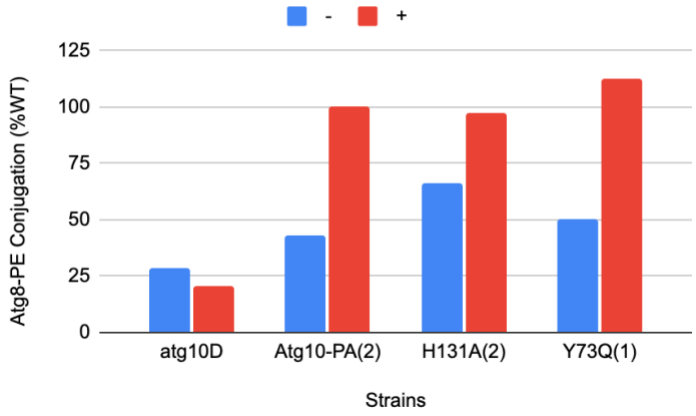

D.

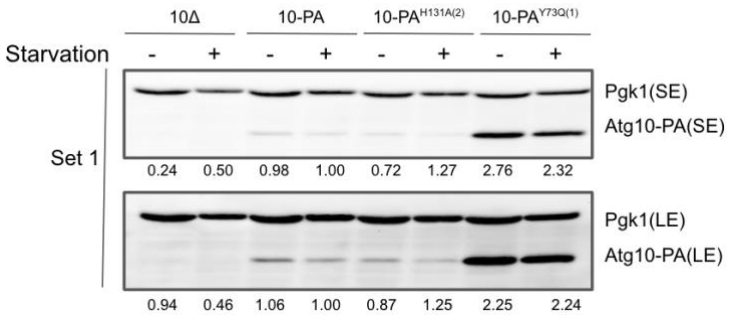

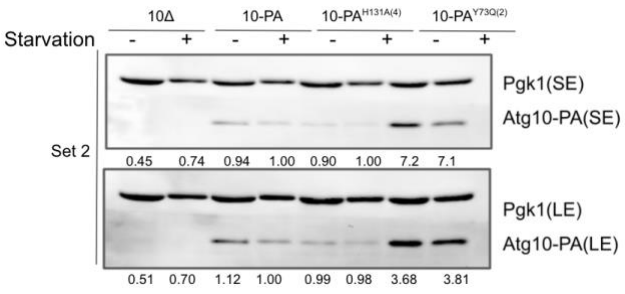

Figure 4. *Atg10 mutants H131A and Y73Q have no significant loss in Atg8-PE conjugation*. (A) Atg10-PA mutants, H131A and Y73Q, were created by site directed mutagenesis and verified by sequencing. (B) The controls, along with the *Atg10-PA* mutants (H131A, Y73Q), were grown in rich medium (-) in log phase and then starved in nitrogen-starvation medium for 3 hours (+). Atg8 and Atg8-PE were analyzed by immunoblotting with anti-Atg8 antibodies. *Atg10-PA* mutants can conjugate Atg8 to lipid PE like the wild-type Atg10-PA. (C) Levels of Atg8 and Atg8-PE were quantified using ImageJ. Then the percentage of Atg8-PE over the total Atg8 was normalized to *Atg10-PA* starved strain. (D) The protein levels of *Atg10-PA* and its mutants were measured by immunoblotting with PAP antibody. Pgk1 was the loading control. A knockout strain *atg10Δ* (10Δ) was the negative control and PA tagged Atg10 (10-PA) was the positive control. A short (SE) and long exposure (LE) of the expression levels of the PA-tagged strains is shown. The Atg10/pGK1 values were normalized to the *Atg10-PA* starved strains.

The levels of PA-tagged mutants were investigated by immunoblotting them with PAP (peroxidase-anti-peroxidase) antibody. The intensity of the *Atg10-PA* bands is very low, indicating that only a small amount of Atg10 protein is present under normal conditions. The Pgk1 was a loading control, and the non-PA tagged strain, WLY176 *atg10Δ,* was the negative control. The H131A mutant expressed at similar levels as the wild-type, *Atg10-PA.* However, the Y73Q mutant showed significant overexpression. This was consisted with the previous study conducted by the Yamaguchi lab, where Y73Q showed overexpressed bands on the western blot (Yamaguchi et al., 2012). We detected the band expression levels with both short and long exposures and measured the ratio of Atg10 and its mutants to the loading control Pgk1. Then we normalized each replicate to *Atg10-PA* starved strains (figure 4D).

Atg10 mutants (H131A, Y73Q) have no significant loss in autophagic activity

To further investigate the *Atg10-PA* mutants, we quantified the autophagic activity by carrying out an ALP assay. The ALP assay is performed in strains with the *pho8Δ60* mutation. In these strains, the alkaline phosphatase Pho8 lacks 60 amino acids so it cannot be transported to the vacuole via the endoplasmic reticulum, and so the only other way it gets to the vacuole is through autophagy. This allows us to measure autophagic activity by determining the amount of

activated alkaline phosphatase (T. Noda & Klionsky, 2008). The ALP assay was carried out on yeast cells containing *Atg10-PA* and mutants in growing and nitrogen-starvation conditions. As shown in figure 5A, there was significantly lower autophagic activity in *atg10Δ* strains, as these lack Atg10 protein. The H131A mutants showed approximately 100% autophagic activity, but the Y73Q mutants showed 60-80% autophagic activity. To further investigate the autophagic activity of these mutants, we analyzed these strains by immunoblotting with an anti-Ape1 antibody. The levels of the cytosolic pre-Ape1 and vacuolar mApe1 were measured. The levels of pre-Ape1 and mApe1 generated by *Atg10-PA* mutants were similar to the wild-type, *Atg10-PA*. The *atg10Δ* strain was the negative control that could not generate a significant amount of the mApe1. We also quantified the levels of pre-Ape1 and mApe1. Upon starvation, the levels of cytoplasmic pre-Ape1 decrease, and mApe1 increase (figure 5B and 5C).

A.

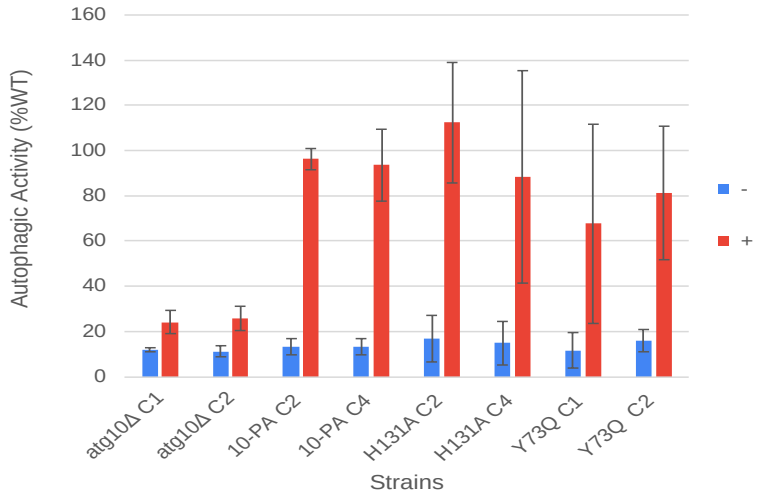

B.

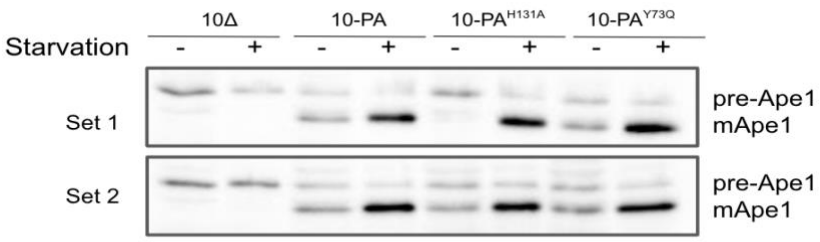

C.

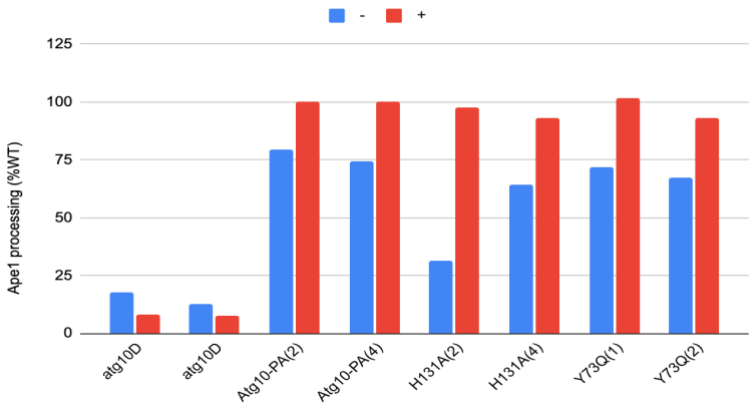

Figure 5: *Atg10 mutants (H131A, Y73Q) rescues autophagic activity.* (A) Pho8Δ60 assay. The knockout strain *atg10Δ* (10Δ) was the negative control and PA tagged Atg10 (10-PA) were the positive controls. The controls, along with the *Atg10-PA* mutants (H131A, Y73Q; two independent clones each), were grown in rich medium (-) in log phase and then starved in nitrogen-starvation medium for 3 hours (+). The autophagic activity of all the strains were quantified by the pho8 Δ60 assay. N=3 replicates, with each replicate independently normalized to the Atg10-PA starved cells. (B) Ape1 processing was analyzed by immunoblotting with anti-Ape1 antibodies. Cells with *Atg10-PA* mutants were able to cleave the pre-Ape1 to form mature Ape1 (mApe1). (C) Levels of pre-Ape1 and mApe1 were quantified using ImageJ. Then the percentage of mApe1 over the total Ape1 was normalized to *Atg10-PA* starved strains.

Discussion

We demonstrated that tagging Atg10 on the C-terminus with PA does not disrupt autophagic function and is suitable for detecting the expression level and the presence of Atg10 by western blot. We also found that both the Atg10 mutants, H131A and Y73Q, retain autophagic activity. Both the mutants had levels of Atg8-PE and Ape1 processing similar to that of the wild type *Atg10-PA*. However, a previous study has found that the mutations H131A and Y73Q decreased the conjugation of Atg12-Atg5 to 30% and 70% compared to the wild-type Atg10, respectively (Yamaguchi et al., 2012). While Atg10 does conjugate Atg12-Atg5 complex, it seems that a partial loss in this conjugation does not correlate with a similar loss in autophagic activity. Hence, a 30% or 70% reduction in Atg12-Atg5 conjugation does not lead to a 30% or 70% reduction in autophagic activity.

Similarly, while Atg10 conjugates Atg8 to lipid PE, a decrease in Atg8-PE conjugation did not correlate with a reduction in autophagic activity or Atg12-Atg5 conjugation. This is shown by our results in figures 5B and C, where mutations in Atg10-PA (H131A and Y73Q) resulted in no defect in Atg8-PE conjugation. Additionally, when we measured the mature Ape1 (mApe1) generated by these mutants, they had less than a 10% reduction in Ape1 processing than the wild type Atg10-PA (figure 4B and C). To further verify these results, we carried out an ALP assay for three replicates and quantified the mean autophagic activity of our mutants. For H131A(2) and H131(4), there was less than a 10% reduction in autophagic activity. For Y73Q(1) and Y73Q(2), there was a 30% and 20% loss of autophagic activity, respectively. However, the error bars for these results were quite large, so more replicates of these mutants need to be tested to get more conclusive evidence regarding a possible partial loss in autophagic activity.

Prior studies have found that in non-selective autophagy, Atg7 activates Atg10 and Atg3. Atg10 conjugates the Atg12-5-16 complex, which upregulates Atg3 by causing a conformational change in Atg3. Atg3 conjugates Atg8 to lipid PE (Cawthon et al., 2018). Studies have shown that Atg7 affects autophagosome size and number, and Atg8 affects autophagosome size (Cawthon et al., 2018; Xie et al., 2008), both of which affect overall autophagic flux. This suggests that the intermediate proteins, Atg3 and Atg10, would also affect the autophagosome size and/or number. For this reason, we hypothesized that Atg10 mutants, H131A and Y73Q, would cause a partial loss in autophagic function. These mutants could be used to investigate the effect on autophagosome size and/or number by transmission electron microscopy (TEM). As our results suggested that H131A and Y73Q largely or completely retain autophagic activity, we can conclude that these single mutants are not suitable for TEM. Some other mutants with partial loss in autophagic function need to be generated. If additional replicates of the Pho8Δ60 assay continue to show the Y73Q mutation causing a 20-30% loss in autophagic activity, we can attempt to construct mutants with a greater loss in autophagic function my introducing other mutations in addition to Y73Q.

As Atg8-PE conjugation is upstream of the formation of the Atg12-5-16 complex, a more direct approach to investigate the effect of Atg10 would be to measure the formation of Atg12-5 conjugation. Currently, we have tagged Atg5 with a Hemagglutinin (HA) Tag. This should allow us to visualize the Atg12-5 conjugation and free Atg5 via western blot. Furthermore, we will also investigate the Atg12-Atg5 conjugation by immunoblotting with anti-Atg12 antibodies. This should also allow us to visualize the Atg12-Atg5 conjugation and the free Atg12 via western blot.

References

Cawthon, H., Chakraborty, R., Roberts, J. R., & Backues, S. K. (2018). Control of autophagosome size and number by Atg7. *Biochemical and Biophysical Research Communications*, *503*(2), 651–656. https://doi.org/10.1016/j.bbrc.2018.06.056

Escobar, K. A., Cole, N. H., Mermier, C. M., & VanDusseldorp, T. A. (2019). Autophagy and aging: Maintaining the proteome through exercise and caloric restriction. *Aging Cell*, *18*(1), e12876. https://doi.org/10.1111/acel.12876

Gatica, D., Lahiri, V., & Klionsky, D. J. (2018). Cargo recognition and degradation by selective autophagy. *Nature Cell Biology*, *20*(3), 233–242. https://doi.org/10.1038/s41556-018-0037-z

Geng, J., & Klionsky, D. J. (2008). The Atg8 and Atg12 ubiquitin-like conjugation systems in macroautophagy. *EMBO Reports*, *9*(9), 859–864. https://doi.org/10.1038/embor.2008.163

Gietz, R. D., & Schiestl, R. H. (2007). High-efficiency yeast transformation using the LiAc/SS carrier DNA/PEG method. *Nature Protocols*, *2*(1), 31–34. https://doi.org/10.1038/nprot.2007.13

Kanki, T., Wang, K., Baba, M., Bartholomew, C. R., Lynch-Day, M. A., Du, Z., Geng, J., Mao, K., Yang, Z., Yen, W.-L., & Klionsky, D. J. (2009). A Genomic Screen for Yeast Mutants Defective in Selective Mitochondria Autophagy. *Molecular Biology of the Cell*, *20*(22), 4730–4738. https://doi.org/10.1091/mbc.e09-03-0225

Longtine, M. S., Mckenzie III, A., Demarini, D. J., Shah, N. G., Wach, A., Brachat, A., Philippsen, P., & Pringle, J. R. (1998). Additional modules for versatile and economical PCR-based gene deletion and modification in Saccharomyces cerevisiae. *Yeast*, *14*(10),

953–961. https://doi.org/10.1002/(SICI)1097-0061(199807)14:10<953::AID-YEA293>3.0.CO;2-U

Lőrincz, P., & Juhász, G. (2020). Autophagosome-Lysosome Fusion. *Journal of Molecular Biology*, *432*(8), 2462–2482. https://doi.org/10.1016/j.jmb.2019.10.028

Martens, S., & Fracchiolla, D. (2020). Activation and targeting of ATG8 protein lipidation. *Cell Discovery*, *6*(1), 23. https://doi.org/10.1038/s41421-020-0155-1

Matoba, K., & Noda, N. N. (2021). Structural catalog of core Atg proteins opens new era of autophagy research. *The Journal of Biochemistry*, *169*(5), 517–525. https://doi.org/10.1093/jb/mvab017

Nair, U., Yen, W.-L., Mari, M., Cao, Y., Xie, Z., Baba, M., Reggiori, F., & Klionsky, D. J. (2012). A role for Atg8–PE deconjugation in autophagosome biogenesis. *Autophagy*, *8*(5), 780–793. https://doi.org/10.4161/auto.19385

Noda, N. N., & Inagaki, F. (2015). Mechanisms of Autophagy. *Annual Review of Biophysics*, *44*(1), 101–122. https://doi.org/10.1146/annurev-biophys-060414-034248

Noda, T., & Klionsky, D. J. (2008). Chapter 3 The Quantitative Pho8Δ60 Assay of Nonspecific Autophagy. In *Methods in Enzymology* (Vol. 451, pp. 33–42). Elsevier. https://doi.org/10.1016/S0076-6879(08)03203-5

Reggiori, F., & Klionsky, D. J. (2013). Autophagic Processes in Yeast: Mechanism, Machinery and Regulation. *Genetics*, *194*(2), 341–361. https://doi.org/10.1534/genetics.112.149013

Ryter, S. W., Cloonan, S. M., & Choi, A. M. K. (2013). Autophagy: A critical regulator of cellular metabolism and homeostasis. *Molecules and Cells*, *36*(1), 7–16. https://doi.org/10.1007/s10059-013-0140-8

Scrivo, A., Bourdenx, M., Pampliega, O., & Cuervo, A. M. (2018). Selective autophagy as a potential therapeutic target for neurodegenerative disorders. *The Lancet Neurology*, *17*(9), 802–815. https://doi.org/10.1016/S1474-4422(18)30238-2

Su, M.-Y., Peng, W.-H., Ho, M.-R., Su, S.-C., Chang, Y.-C., Chen, G.-C., & Chang, C.-I. (2015). Structure of yeast Ape1 and its role in autophagic vesicle formation. *Autophagy*, *11*(9), 1580–1593. https://doi.org/10.1080/15548627.2015.1067363

Wang, C.-W., & Klionsky, D. J. (2003). The Molecular Mechanism of Autophagy. *Molecular Medicine*, *9*(3–4), 65–76. https://doi.org/10.1007/BF03402040

Wu, M.-Y., Song, J.-X., Wang, S.-F., Cai, C.-Z., Li, M., & Lu, J.-H. (2018). Selective autophagy: The new player in the fight against neurodegenerative diseases? *Brain Research Bulletin*, *137*, 79–90. https://doi.org/10.1016/j.brainresbull.2017.11.009

Xie, Z., & Klionsky, D. J. (2007). Autophagosome formation: Core machinery and adaptations. *Nature Cell Biology*, *9*(10), 1102–1109. https://doi.org/10.1038/ncb1007-1102

Xie, Z., Nair, U., & Klionsky, D. J. (2008). Atg8 Controls Phagophore Expansion during Autophagosome Formation. *Molecular Biology of the Cell*, *19*(8), 3290–3298. https://doi.org/10.1091/mbc.e07-12-1292

Yamaguchi, M., Noda, N. N., Yamamoto, H., Shima, T., Kumeta, H., Kobashigawa, Y., Akada, R., Ohsumi, Y., & Inagaki, F. (2012). Structural Insights into Atg10-Mediated Formation of the Autophagy-Essential Atg12-Atg5 Conjugate. *Structure*, *20*(7), 1244–1254. https://doi.org/10.1016/j.str.2012.04.018

Yin, Z., Pascual, C., & Klionsky, D. (2016). Autophagy: Machinery and regulation. *Microbial Cell*, *3*(12), 588–596. https://doi.org/10.15698/mic2016.12.546